MULTI-SCALE CORRELATION IN TURBULENT OPEN-CHANNEL GRAVEL-BED RIVER FLOWS

Mário J. Franca[1], Rui M.L. Ferreira[2], & Ulrich Lemmin[3]

[1] Faculty of Sciences and Technology & IMAR – CMA, New University of Lisbon, Portugal, Quinta da Torre, 2829 Caparica
[2] CEHIDRO & Instituto Superior Técnico, Technical University of Lisbon, Portugal, Av. Rovisco Pais, 1049 Lisbon
[3] ENAC, École Polytechnique Fédérale de Lausanne, Switzerland, CH 1015 Lausanne
E-mail: mfranca@fct.unl.pt

Abstract

In natural low relative submergence flows over gravel beds, different length scales exist simultaneously, ranging from grain configuration- to channel configuration-scales. Consequently, a wide range of time-scales co-exist which may be analyzed in an Eulerian frame. By taking into account the interaction between scales, the formal theoretical framework of these flows renders more complex. The present research contributes towards a multi-scale analysis of river flows by studying the cross-correlation partition between eddy-scales in several flow layers. The present study is based on 15 instantaneous 3D velocity profiles that were measured by means of an ADVP with a vertical resolution of 5 mm in a 0.30 x 0.40 m^2 horizontal grid for 3.5 min each with an acquisition frequency of 26 Hz. Flow structures were isolated and characterized by their time-scales by means of conditional sampling techniques and wavelet multilevel decomposition of single point instantaneous velocity measurements. For this analysis, an eight wavelet decomposition was applied to velocity measurements in a gravel-bed river with low relative submergence (h/D_{50} = 2.9). The cross-correlation between the isolated structures and the remaining signal was estimated. The global contribution of a particular scale to total normal stresses and also to local stresses within one coherent structure phase cycle is thus examined and analyzed.

Introduction

River flows are affected by a wide range of coexisting flow scales that are related to grain roughness (grain-scale), bed-forms (river width-scale), protuberant elements (grain-scale to river width-scale, this is especially important in low relative submergence flows), and channel configuration (valley-scale, e.g., bends, braiding). Therefore, modeling these flows is complex. Nikora (2008) presents a power spectrum which represents all the time scales within river flows, ranging from turbulent or small scale phenomena, scaling with seconds or even shorter periods, to large-scale phenomena scaling with seasons or even years. However, few researchers have addressed the interaction of these scales.

Progress in analyzing and modeling heterogeneous and irregular-bounded river flows has been made by applying upscaling techniques such as double-averaging to the conservation equations (Smith & McLean 1977; Nikora et al. 2001; Ferreira et al. 2009). However, such techniques may prove insufficient in time varying flows with boundary irregularities that are characterized by two or more distinct time scales. Cross correlations between different time scales may introduce additional resistance and/or stress terms into the conservation equations. In the case of two distinct roughness scales, attempts have been made to separate "micro" and "macro" form-induced stresses (Poggi et al. 2008), or for the TKE equation, to separate production in large-scale and wake-scale bands (Poggi et al. 2004). At present, no formal theoretical framework or closure models are available for the general case of multiple scales, which remains an open subject in the understanding of river flows.

Although it is essential to understand those fluvial processes that cannot be reproduced in the laboratory, few field investigations in natural or canalized rivers such as the present one have been published (Buffin-Bélanger and Roy 2005). The present investigation uses field data in a first step towards an integrated analysis of multi-scale processes in highly heterogeneous turbulent flows, where conservation equations should take into account cross correlation between different scales present in the flow.

The present field data set was analyzed by means of wavelet transforms to detect and reconstruct the productive coherent structures (Franca & Lemmin 2006a). Wavelet analysis is a suitable tool for the study of turbulence in geophysical flows, particularly for multi-mode decomposition of instantaneous signals and scale-conditional sampling techniques (Foufoula-Georgiou & Kumar 1994).

In the same river, at the same site, although for a different experimental configuration, an analysis of similar data was performed for time-averaged and double-averaged turbulent structure of the flow (Franca *et al.* 2008). Based on this experience, and using Huang's empirical mode

decomposition combined with the Hilbert transform (Huang *et al*. 1998), the authors could identify and reconstruct large-scale structures longitudinally scaling with 3 to 7 times the water depth (Franca & Lemmin 2008).

Previous work using the present data concerned the identification of coherent structures existing within narrow reaches of the flow energy spectra. Here, a multiple-scale analysis is carried out where the interaction between different scale bands becomes evident and can be characterized and quantified. Conditional sampling techniques and the wavelet multilevel decomposition of single point instantaneous velocity measurements are used to isolate the signal corresponding to a particular scale. The global contribution of a particular scale to total normal stresses and also to local stresses within one coherent structure phase cycle is examined.

3D Acoustic Velocity Profiler (ADVP) measurements were performed in an armored gravel-bed river with a relative submergence of $h/D_{50} = 2.9$ and a wide range of bottom roughness element sizes; h = mean flow depth, D_{50} = bed grain size diameter for which 50% of the grains have a smaller diameter. The velocity data is filtered within the scale band, as defined in Franca and Lemmin (2006a) for the most energetic scales present in the flow, based on an eight wavelet decomposition of the velocity signal. Subsequently, cross-correlation between the sampled data and the residual signal is analyzed and discussed.

Following this introduction, the theoretical framework that considers the interaction between scales in the flow is presented. Thereafter, measurement details are given, the results are presented and discussed, and finally, the main conclusions are drawn.

Theoretical Framework

Reynolds decomposition accounts for the instantaneous fluctuation of a generic variable θ in turbulent flow fields:

$$\theta = \bar{\theta} + \theta', \text{ where } \bar{\theta'} = 0 \tag{1}$$

The prime denotes instantaneous fluctuations and the overbar indicates time-averaging (Hinze 1975). The application of Reynolds decomposition to velocities and its introduction to Navier-Stokes equations, followed by the application of the time-averaging operator, results in the so-called Reynolds-averaged Navier-Stokes equations (RANS) which, for 3D, isothermal, steady turbulent open-channel flows of incompressible Newtonian fluids with no solid discharge, may be expressed using the following Cartesian tensor notation (Hinze 1975):

$$\overline{u_\iota}\frac{\partial \overline{u_\jmath}}{\partial x_i} = g_j - \frac{1}{\rho}\frac{\partial \bar{p}}{\partial x_j} + \frac{\partial}{\partial x_i}\left(\upsilon\frac{\partial \overline{u_\jmath}}{\partial x_i} - \overline{u'_\jmath u'_\iota}\right) \tag{2}$$

where u stands for velocity, x, for space variable; subscripts i and j are the 3D Cartesian directions with 1 for streamwise, 2 for spanwise and 3 for vertical ($\{x, y, z\} \equiv \{1, 2, 3\}$), g is the gravity acceleration, ρ, fluid density, p, pressure, and ν is the fluid kinematic viscosity. The term on the left hand side represents the mean momentum variation due to convection. Total mean stresses per flow density, τ_{ij}/ρ, are divided into viscous and turbulent or Reynolds stresses; these are the left and right hand side terms within the brackets, respectively. Reynolds stresses per fluid density correspond to the second order moments of turbulent velocities.

To incorporate the influence of a single flow scale λ, in the remaining velocity components, a new decomposition of turbulence is suggested,

$$\theta' = \langle\theta'\rangle_\lambda + \theta'', \text{ where } \overline{\langle\theta'\rangle_\lambda + \theta''} = 0 \tag{3}$$

$$\theta = \bar{\theta} + \langle\theta'\rangle_\lambda + \theta'' \tag{4}$$

where square brackets indicate the signal mode associated to a particular flow scale and double prime, the residual signal (hereinafter referred to as "residue"). Regarding second order moments which represent Reynolds stresses in eq. 2, the application of multi-scale decomposition (4) results in,

$$\overline{u'_\jmath u'_\iota} = \underbrace{\overline{\langle u'_\iota\rangle_\lambda\langle u'_\jmath\rangle_\lambda}}_{I} + \underbrace{\overline{\langle u'_\iota\rangle_\lambda u''_\jmath} + \overline{u''_\iota\langle u'_\jmath\rangle_\lambda}}_{II} + \underbrace{\overline{u''_\iota u''_\jmath}}_{III} \tag{5}$$

In (5), cross correlation between scale ranges becomes apparent in term II, whereas auto-correlations within scale ranges correspond to terms I and III. The decomposition of Reynolds stresses in (5) allows the evaluation of the interaction between scale ranges and, for example, the control of smaller scale processes by large-scale events.

The present analysis is a first step towards an integrated analysis of multi-scale processes in highly heterogeneous turbulent flows, where conservation equations should take into account cross correlation between different scales. Presently we only quantify second order moments in the streamwise direction (streamwise normal stresses) throughout the water column, namely the relationship between the most energetic scale identified previously

(Franca & Lemmin 2006a) and the residue of the velocity signal for each point measurement. A coherent structure detection technique based on wavelet multiresolution analysis was developed, conditioned by event scale and amplitude. It was applied to detect and reconstruct coherent structures scaling with the most energetic scale present in the measured time series. The length of the most energetic coherent structures corresponds to a macro scale with an order of magnitude situated between a characteristic bed grain dimension ($\approx D_{50}$) and the water depth (h). Its value is around $\lambda = 0.43$ - 0.86 s (in length scale, $\Lambda \approx 0.10$ to 0.20 m). An N = 8 level wavelet decomposition with the Daubechies type D4 function (Daubechies 1988) was used to describe the energy partition throughout the different structure scales present in the flow and was then taken as the base to isolate the mode corresponding to the most energetic scale.

In the present investigation, we assessed experimentally instantaneous velocities throughout the water column in 15 different profiles; with these we estimated, in eq. 5, $\overline{u'_1{}^2}(z)$, $\overline{\langle u'_1\rangle_\lambda{}^2}(z)$, $\overline{\langle u'_1\rangle_\lambda u''_1}(z)$ and $\overline{u''_1{}^2}(z)$. λ corresponds to the most energetic scale at one measuring point that is equal to 0.53 s when averaged over all the measured velocities.

Measuring Details

A field deployable ADVP developed at the EPFL allows measuring 3D quasi-instantaneous velocity profiles over the entire depth of the river flow. Its resolution permits evaluating the main turbulent flow parameters. Details of the ADVP working principle are given in Rolland & Lemmin (1997). We used a configuration of the ADVP consisting of four receivers and one emitter that provides one redundancy in the 3D velocity profile measurements. This redundancy is used for noise elimination and data quality control (Hurther & Lemmin 2000b, Blanckaert & Lemmin 2006). This configuration combined with a dealiasing algorithm developed by Franca & Lemmin (2006b) theoretically allows noise-free 3D instantaneous velocity cross-correlation estimates. A Pulse Repetition Frequency (PRF) of 1666 Hz and a Number of Pulse Pairs (NPP) of 64 were used to estimate the Doppler shift, resulting in a sampling frequency of 26 Hz. A bridge which supported the ADVP instrument allowed the easy displacement of the system across the river section and along the river in the streamwise direction, thus minimizing ADVP vibration and flow disturbance.

The present measurements were taken during the summer of 2004, in the Swiss river Venoge (canton of Vaud). 15 instantaneous velocity profiles (Fig. 1) were measured in a single day under stationary shallow water flow conditions, as confirmed by the discharge data provided by the Swiss Hydrological and Geological Services. The measuring station was located about 90 m upstream of the Moulin de Lussery. River hydraulic characteristics at the time of the measurements are shown in Table 1.

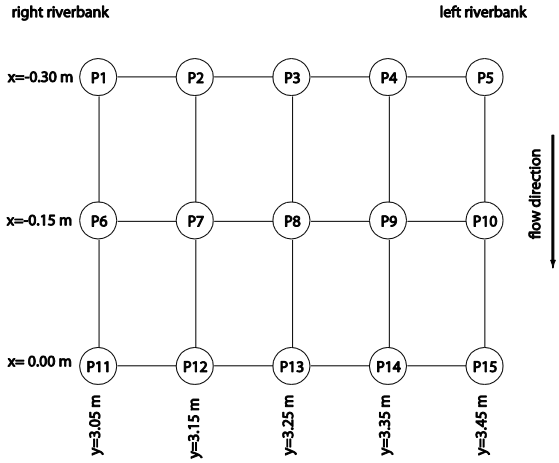

Figure 1: Measuring grid: plane view (spanwise distances are measured from the right riverbank)

Table 1: Summary of the river hydraulic characteristics

Q (m^3/s)	0.76
s (%)	0.33
h (m)	0.20
B (m)	6.30
Re ($x10^4$)	12
Fr (-)	0.4
D_{50} (mm)	68
D_{84} (mm)	89
h/D_{50} (-)	2.94

In Table 1, Q is discharge, s is river slope, h is water depth, B is river width, Re is Reynolds number, Fr is Froude number, and D_{50} and D_{84} are bed grain size diameters for which 50% and 84% of the grain diameters are respectively smaller. The water depth, h, is the distance between the water surface and the lowest trough in the riverbed. The riverbed material was sampled according to the Wolman method (Wolman, 1954), and analysed using standard sieve sizes to obtain the weighted grain size distribution.

The riverbed is hydraulically rough and composed of coarse and randomly spaced gravel. No sediment transport occurred during the measurements. The measurements were made on a 3 x 5 rectangular horizontal grid (x-y). The velocity profiles were equally spaced in the spanwise direction with a distance of 10 cm, and in the streamwise direction with a distance of 15 cm. The vertical resolution of the measurements is about 0.5 cm and the number of gauges per profile ranges from 22 to 37. The total 3D grid had 454 gauge points, making a measuring density of roughly 0.4 points/cm^3. The level of the riverbed was

determined by the sonar-backscattered response. Profile data were recorded for 3.5 min in each position.

Results

The instantaneous streamwise velocity series measured at each point of the profiles in Fig. 1 were decomposed using an eight-level wavelet analysis. At each point (from the 454 gauges), two velocity series were reconstructed. The first corresponded to the mode (or scale – λ) with most of the energy within the signal – $\langle u'_1\rangle_\lambda$, and the second one corresponded to the residue – u''_1. We thus estimated second order moments from eq. 5: term I, $\overline{\langle u'_1\rangle_\lambda^2}$; term II, $\overline{\langle u'_1\rangle_\lambda u''_1}$; and, term III, $\overline{u''_1{}^2}$; hereinafter referred to as scale autocorrelation, cross-moment, and residue autocorrelation, respectively. Coherent structures scaling with λ were subsequently sampled in the signal $\langle u'_1\rangle_\lambda$ and, through phase averaging techniques based on a Hilbert transform of the velocity signal (Huang *et al.*, 1998), we were able to reconstruct instantaneous quantities $\langle u'_1\rangle_\lambda^2$, $u''_1{}^2$ and $\langle u'_1\rangle_\lambda u''_1$ within one coherent structure cycle. We were thus able to estimate phase-sampled scale autocorrelation $\overline{\overline{\langle u'_1\rangle_\lambda^2}}$, phase-sampled cross-moment $\overline{\overline{\langle u'_1\rangle_\lambda u''_1}}$, phase-sampled residue autocorrelation $\overline{\overline{u''_1{}^2}}$ and phase-sampled streamwise Reynolds normal stress $\overline{\overline{u'_1{}^2}}$. For the subsequent analysis we chose one cycle over which the quantity $\overline{\overline{\langle u'_1\rangle_\lambda u''_1}}$ was maximum. Four types of results are discussed in the following.

Fig. 2 shows measured Reynolds normal stress profiles (per ρ), in the streamwise, spanwise, and vertical Cartesian directions, time-averaged over the entire measuring period. All profiles are referenced to the lowest bed elevation. Positions in the measured grid are indicated in the figure (compare Fig. 1 for locations). The two horizontal lines represent the level of the highest crests in the riverbed and the local riverbed level, respectively.

Some heterogeneity is found in the amplitude of time-averaged stresses, especially in the vertical component, but generally they all show similar distribution patterns. Compared to deep flow conditions, the macro roughness of the riverbed induces major changes in the turbulence structure.

Normal streamwise stresses increase from the free surface until roughly to the limit of the crests. Below, streamwise stress distribution is determined by local effects of the randomly distributed bed forms. Spanwise normal stress distributions have a convex shape. In most cases, they reach their maxima slightly below z/h = 0.60; in a few profiles, the peak of spanwise normal stress is attained within the troughs and crests of the riverbed. Vertical stress distributions also have a convex shape, and the maximum is generally reached close to the middle of the water depth.

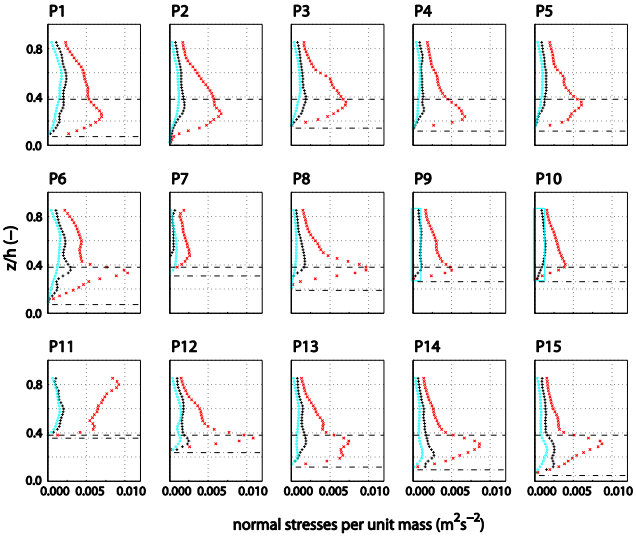

Figure 2: Measured profiles of Reynolds normal stresses per ρ a) streamwise (red), b) spanwise (black), and c) vertical (blue). The dashed horizontal line represents the normalized height z/h = 0.38 corresponding to the highest crests of the riverbed and the lower dashed-dotted line indicates the local bottom level.

From Fig. 3, the contribution of the cross-moment component to the total normal stresses is shown to be negligible.

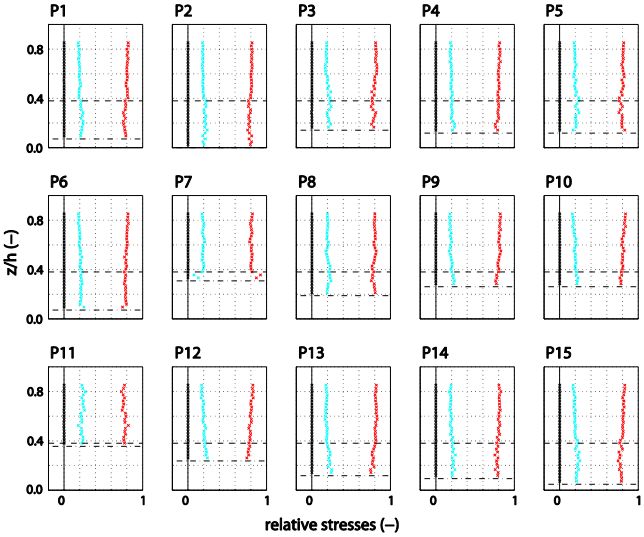

Figure 3: For the streamwise direction: Profiles of contributions of scale autocorrelation ($\overline{\langle u'_1\rangle_\lambda^2}$; blue), cross-moment ($\overline{\langle u'_1\rangle_\lambda u''_1}$; black), and residue autocorrelation ($\overline{u''_1{}^2}$; red) to total Reynolds stress $\overline{u'_1{}^2}$.

Scale and residue autocorrelation proved to be the main components of the total Reynolds stresses. They are complementary as expected from eq. 5. Scale autocorrelation represents, roughly and consistently over the 15 measured profiles, about 20% of the total energy of

the flow. This fraction remains constant over all the measured points, independent of the scale corresponding to the most energetic eddies which varies in space.

For an individual event, sampled and reconstructed as described above, the balance between scale autocorrelation, cross-moment and residue autocorrelation (Fig. 4) is similar to time-averaged information in Fig. 3. Nevertheless, an instantaneous visualization shows the cross influence between $\langle u'_1 \rangle_\lambda$ and u''_1 changing instantaneously the balance between scale and residue autocorrelations; negative instantaneous values of cross-correlation exists within one coherent structure cycle. Phase-sampled cross-moment however are never higher than 0.2 of the total phase-sampled energy.

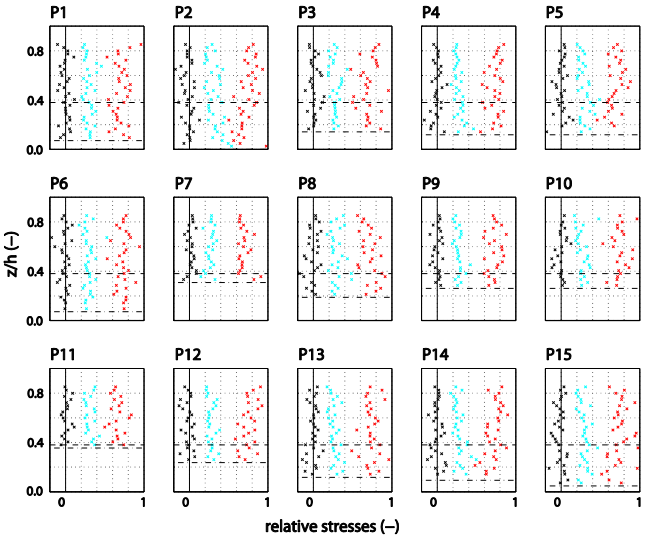

Figure 4: For the streamwise direction: Profiles of the contributions of phase-sampled scale autocorrelation ($\overline{\langle u'_1 \rangle_\lambda^2}$; blue), cross-moment ($\overline{\langle u'_1 \rangle_\lambda u''_1}$; black), and residue autocorrelation ($\overline{u''^2_1}$; red) to Reynolds stress ($\overline{u'^2_1}$), within one event.

Fig. 5 compares correlations obtained within individual coherent events and total Reynolds stresses (note, here the values are not complementary of the total Reynolds stress). Again, the residue autocorrelation represents higher energy than the scale autocorrelation. However the latter appears to be relatively more important when looking within individual events. Phase-sampled cross-moments dominate over those averaged over the entire record (Fig. 2) and are either negative or positive. Higher peaks occur within troughs and crests of the riverbed and generally $\overline{\langle u'_1 \rangle_\lambda u''_1}$ range between -0.2 and 0.2.

Conclusions

The present results are a first step towards a multi-scale analysis of turbulent processes in highly heterogeneous turbulent river flows. Based on wavelet multi-level analysis, we decomposed instantaneous velocity fields over 15 different profiles in order to identify the most energetic scale of each measuring point. Then, we evaluated the autocorrelation of the most energetic modes and the residue and the cross-correlation between the two.

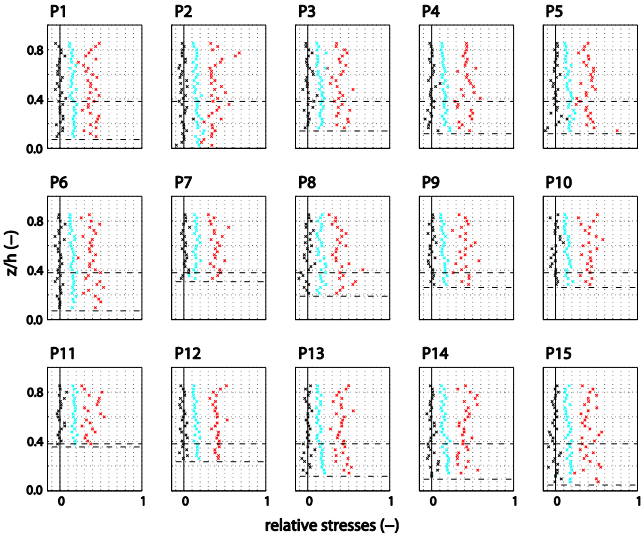

Figure 5: Measured profiles of streamwise normal Reynolds stresses relative to time-averaged total stresses; contribution of one coherent structure cycle from the sampled scale ($\overline{\langle u'_1 \rangle_\lambda^2}$; blue), the residue ($\overline{u''^2_1}$; red) and the crossed component $\overline{\langle u'_1 \rangle_\lambda u''_1}$ (black).

We tried to quantify the interaction between scales within the flow turbulent structure. For time-averaged quantities, cross-moments between energetic scales and residue are insignificant and negligible. However, for individual coherent events, these crossed interactions acquire importance for the local flow energy. Cross-moments are never higher than 0.2 of the total signal energy.

The results show the importance of the averaging window for each flow analysis and indicate that further sampling and correlation techniques have to be applied to determine the interaction between scales. In the future, the formal introduction of multiple-scale decomposition (eq. 4 and 5) into transport equations, with the development of new terms accounting for interaction between scales, is envisaged.

Acknowledgments

The authors acknowledge the financial support of the Portuguese Science and Technology Foundation (PTDC/ECM/099752/2008).

References

Daubechies, I. (1988). Orthonormal bases of compactly supported wavelets. Comm. Pure Appl. Math. XLI: 909-996.

Blanckaert, K. & Lemmin, U. (2006). Means of noise reduction in acoustic turbulence measurements. J. Hydr. Res. 44, 3-17.

Buffin-Bélanger, T. & Roy, A.G. (2005). 1 min in the life of a river: selecting the optimal record length for the measurement of turbulence in fluvial boundary layers. Geomorphology 68, 77-94.

Ferreira, R.M.L., Ferreira, L.M., Ricardo, A.M. & Franca, M.J. (2009). Impacts of sand transport on flow variables and dissolved oxygen in gravel-bed streams suitable for salmonid spawning. River Res. and Appl. Vol. 26(4) 414-438.

Foufoula-Georgiou, E. & Kumar, P. (1994). Wavelets in geophysics, San Diego: Academic Press.

Franca, M.J. & Lemmin, U. (2006a). Detection and reconstruction of coherent structures based on wavelet multiresolution analysis. in Ferreira R.M.L., Alves E., Leal, J.G.B. and Cardoso A.H. (Eds) River Flow 2006 - 3th Int. Conf. on Fluvial Hydraulics, Lisbon, Portugal, September 2006, pp.153-162.

Franca, M.J. & Lemmin, U. (2006b). Eliminating velocity aliasing in acoustic Doppler velocity profiler data. Meas. Sci. Technol. 17, 313-322.

Franca, M.J. & Lemmin, U. (2008). Using empirical mode decomposition to detect large-scale coherent structures in river flows. in Altinakar, M.S., Kokpinar, M.A., Aydin, I., Cokgor, S., and Kirkgoz, S. (Eds.) River Flow 2008 - 4th Int. Conf. on Fluvial Hydraulics, Cesme, September 3 – 5, 2008, pp. 67-74.

Franca, M.J., Ferreira, R.M.L. & Lemmin, U. (2008). Parameterization of the logarithmic layer of double-averaged streamwise velocity profiles in gravel-bed river flows. Adv. Water Res. 31, 915–925.

Hinze, J.O. (1975). Turbulence. Cambridge (Ma): McGraw-Hill.

Huang, N.E., Shen, Z., Long, S.R., Wu, M.C., Shih, H.H., Zheng, Q., Yen, N.C., Tung, C.C. & Liu, H.H. (1998). The empirical mode decomposition and the Hilbert spectrum for nonlinear and non-stationary time series analysis. Proc. R. Soc. Lond. A, 454, 903-995.

Hurther, D. & Lemmin, U. (2000). Shear stress statistics and wall similarity analysis in turbulent boundary layers using a high-resolution 3D ADVP. IEEE J. Oc. Eng. 25(4): 446-457.

Nikora, V.I., Goring, D.G., McEwan, I.K. & Griffiths, G. (2001), Spatially averaged open-channel flow over rough bed, J. Hydraul. Eng. 127(2) 123-133.

Nikora, V. (2008). Hydrodynamics of gravel-bed rivers: scale issues. in Habersack H., Piegay H. and Rinaldi M., "Gravel-bed rivers VI: From Process Understanding to River Restoration", Elsevier, 61-81.

Poggi, D. & Katul, G.G. (2008). Micro- and macro-dispersive fluxes in canopy flows. Acta Geoph. 56, 778-800.

Poggi, D., Katul, G.G. & Albertson, J.D. (2004). A note on the contribution of dispersive canopy fluxes to momentum transfer within canopies. Boundary Layer Meteorology 111, 615-621.

Rolland, T. & Lemmin, U. (1997). A two-component acoustic velocity profiler for use in turbulent open-channel flow. J. Hydr. Res. 35(4) 545.

Smith, J.D., & McLean, S.R. (1977). Spatially averaged flow over a wavy surface. J. Geophys. Res. 83(12) 1735-1746.

Wolman, M.G. (1954). A method of sampling coarse river-bed material. Tran. Amer. Geop. U. 35(6) 951.